Multiobjective Optimization of Cyclone Separators Using Genetic Algorithm

G. Ravi, Santosh K. Gupta,† and M. B. Ray*

Department of Chemical and Environmental Engineering, National University of Singapore, 10 Kent Ridge Crescent, Singapore 119260

Multiobjective optimization of a set of N identical reverse-flow cyclone separators in parallel was carried out by using the nondominated sorting genetic algorithm (NSGA). Two objective functions were used: the maximization of the overall collection efficiency and the minimization of the pressure drop. Nondominated Pareto optimal solutions were obtained for an industrial problem in which 165 m^3/s of air was treated. In addition, optimal values of several decision variables, such as the number of cyclones and eight geometrical parameters of the cyclone, are obtained. The study shows that the diameters of the cyclone body and the vortex finder, and the number of cyclones used in parallel, are the important decision variables influencing the optimal solutions. This study illustrates the applicability of NSGA in solving multiobjective optimization problems involving gas−solid separations.

Introduction

Cyclone separators have been used extensively during this century as a major gas-cleaning device. The standard designs available now were perfected decades ago on the basis of practical experience and insight but often without quantitative application of the principles of engineering practice. Although these approaches have worked well in certain circumstances, they may not always lead to the best possible designs. Now, increasing demands and competition require the use of good mathematical models describing the operation of cyclones, as well as their use, with modern tools of optimization to give the best designs. In this work, we present the methodology for obtaining the "best" designs for cyclones that optimize (maximize or minimize) *several* performance criteria (objective functions) *simultaneously*. A simple but robust, AI-based technique (genetic algorithm, GA) is used with a good mathematical model to obtain optimal designs.

It is well-known that the results of any optimization study are as good as the quality of the model of the processes involved. Fortunately, several theoretical models[1−9] are available in the open literature for calculating the grade efficiency, and subsequently the overall collection efficiency, η_o, of cyclones. These models perform with varying degrees of success. In effect, most of them perform adequately for particles larger than about 10 μm. Salcedo[10] compared the grade efficiencies calculated using several models[4,5,8,9] and found that the model of Mothes and Löffler[8] provides good estimates for both the grade-efficiency curves and the particle size distributions of the cyclone catch and/or outlet dusts. Our own[11,12] earlier experience with the model of Mothes and Löffler[8] is similar. We have, therefore, used this model[8] in the present study.

In addition to the overall collection efficiency, another important performance characteristic of cyclones is the pressure drop, Δp, which is related to the energy costs. Several expressions have been developed[1,8,13−15] to predict Δp, and most of the models express Δp in terms of the number, ΔH, of inlet velocity heads of the gas.

$$\Delta p = \frac{1}{2}\rho_g v_i^{\,2}(\Delta H) \tag{1}$$

The value of ΔH is usually a constant for geometrically similar cyclones of different diameters. Conflicting inferences[16−18] on the suitability of different models have been reported. In our work, we have chosen the model of Shepherd and Lapple[13] for predicting Δp because of its simplicity and relatively higher accuracy.[17,18]

$$\Delta H = \frac{16ab}{D_e^{\,2}} \tag{2}$$

In sharp contrast to work on the modeling of cyclones, relatively little work has been reported[18−21] on their optimization. Muschelknautz[19] used models[1,22,23] to obtain two geometrical ratios, (H/D_e) and (D/D_e), for the optimized cyclone, which resulted in the desired overall collection efficiency with minimum pressure drop. Unfortunately, this study did not predict *all* of the dimensions of the optimized cyclone. Leith and Mehta[18] developed a procedure by which the designer determined the set of geometrical ratios that gave the highest possible efficiency for any combination of gas throughput, cyclone diameter, and pressure drop. Dirgo and Leith[20] varied the outlet diameter of the Stairmand cyclone and searched for compensating changes among other cyclone dimensions in order to increase the efficiency without changing the pressure drop. In both of these studies,[18,20] the pressure drop is fixed, and the cyclone dimensions are changed to achieve the maximum value of η_o. Ramachandran et al.[21] predicted the minimum pressure drop and the geometrical ratios of

* Author to whom correspondence should be addressed. E-mail: cheraym@nus.edu.sg. Fax: (65) 779 1936.

† Present address: Department of Chemical Engineering, University of Wisconsin, Madison, WI 53706. On leave from the Indian Institute of Technology, Kanpur 208016, India.

10.1021/ie990741c CCC: $19.00 © 2000 American Chemical Society
Published on Web 10/11/2000

the optimized cyclone for a given aerodynamic cut diameter, d_{50}.

In all of the earlier optimization studies, a single objective function was used. However, optimization of cyclones really involves several conflicting objectives, namely, maximization of the overall collection efficiency and minimization of both the pressure drop and the cost. To the best of our knowledge, such a multiobjective optimization study on cyclones has not been reported in the open literature. In this study, optimization of cyclones (at the design stage) is carried out using multiple (conflicting) objective functions, using a genetic algorithm.

Genetic algorithms were introduced by Holland[24] in 1975 and represent a nontraditional search and optimization method. They mimic the principles of genetics and natural selection to develop search and optimization procedures. Simple genetic algorithms (SGAs) are suitable for optimization problems involving single objective functions. In such problems, a SGA usually gives all of the global optima present. In contrast, for problems involving multiple objective functions, *unique* optimal solutions may not exist, and there may exist a set of several equally desirable, optimal points. These solutions are referred to as Pareto sets or nondominated solutions. None of these nondominated solutions is superior to any of the other points, and indeed, any one of them could be selected for design or operation. The choice of a "preferred" solution from among the Pareto set of points requires additional knowledge about the problem, information that may be intuitive and hence, nonquantifiable. Statistical techniques using the opinions of several decision makers are often used to arrive at the preferred solution.[25] However, the Pareto set assists in narrowing down the choices to be considered for a decision maker and so is of immense importance.

The classical method that has been used, until recently, to solve problems involving several objectives involves combining the objectives into a single scalar objective function, a weighted average of the several objectives. This *scalarization* of the actual problem allows a simpler optimization algorithm to be used. Unfortunately, the solution obtained depends largely on the values of the weighting factors used, which may not be known unequivocally. In addition, one of the drawbacks with this approach is that some solutions may be missed during solution.[26] The advent of powerful computers has now made it possible to solve problems that involve the optimization of an objective function, **I**, that is a vector of several objectives, I_i. Several techniques are available[25] for solving such multiobjective optimization problems. One robust technique, which works with a population of solutions, generated randomly, is an adaptation of a SGA[24,27,28] and is known as the nondominated sorting genetic algorithm (NSGA).[28−30] In this technique, the trial solutions, known as chromosomes or strings, are classified into several fronts on the basis of the concept of nondominance and assigned appropriate fitness values.[29,30] The techniques of SGA are then used to obtain the Pareto optimal set. A short summary of NSGA is provided in the Appendix.[31]

Formulation

The model of Mothes and Löffler[8] and the computer code developed for evaluating η_o were first tested on some experimental data[11] obtained with a Stairmand[7] cyclone having a diameter $D = 0.4$ m. The dimensions and the specifications of the feed to the cyclone for one set of experimental conditions are given in Table 1. A vane at the inlet was used to vary the value of b/D, consequently producing different inlet velocities, v_i, while keeping the inlet flow rate, Q, constant. The experimental data[11] obtained using the system described in Table 1 are shown in Figure 1a for three values of the input velocities, v_i (and b/D). The grade efficiency, $\eta(D_p)$, curves predicted by the model of Mothes and Löffler[8] are obtained using the model equations summarized in Table 2 (eqs A1−A19). These are also plotted in Figure 1 for the three different values of v_i. The importance of v_i in cyclone operation is well-known as it influences both the pressure drop and the collection efficiency. Only a single curve-fit parameter, the effective mean particle diffusivity, D_s, in the turbulent gas flow in the cyclone, has been used to generate the model-predicted curves. Values of D_s between 5×10^{-4} and 10^{-3} m^2/s were found to represent the data reasonably well, as shown in Figure 1b. These values for the diffusivity are lower than the value of 0.0125 m^2/s prescribed by Mothes and Löffler.[8] In all cases, the shapes of the experimental curves are predicted quite well by the model. However, the absolute positions differ slightly for particles below 5 μm and warrant further improvement.

Table 1. Details of the Cyclone and Feed Used in One Experiment[11]

specifications	value
Cyclone	
number of cyclones, N	1
D, m	0.4
D_e/D	0.5
B/D	0.375
H/D	4.0
S/D	0.5
h/D	1.2
a/D	0.5
b/D	0.069, 0.093, 0.135
Feed	
inlet velocity, v_i, m/s	21.7, 16, 11
inlet flow rates, Q, m^3/s	0.1194
mass-mean diameter of solids,[a] D_p, μm	3.55
standard deviation of size distribution of solids,[a] σ_p	0.21
Properties and Parameters	
density of gas, ρ_g, kg/m^3	1.14
viscosity of gas, μ_g, Pa s	18×10^{-6}
density of solids, ρ_s, kg/m^3	2700
effective mean diffusivity of solids in gas, D_s, m^2/s	10^{-3}

[a] Size distribution of solids in feed (log-normal):

$$m_{in}(D_p) = \frac{1}{\sqrt{2\pi} D_p \ln \sigma_p} \exp\left[-\frac{(\ln D_p - \ln \bar{D}_p)^2}{2(\ln \sigma_p)^2}\right]$$

In our optimization study, in addition to computing values of η_o, we also need to evaluate values for the pressure drop, Δp, in the cyclone, as well as the total annual cost, C_o. As mentioned earlier, we have chosen the Shepherd and Lapple[13] model for estimating the pressure drop, and the exact equations used are given in Table 2 (eqs A20 and A25). The cost for single and multiple cyclones is calculated using an adaptation of the correlations of Vatavuk[32] and Crawford.[33] The available correlations for C_o have been developed only for cyclones having the standard geometry[7] (with the contribution of the fixed cost to C_o represented in terms

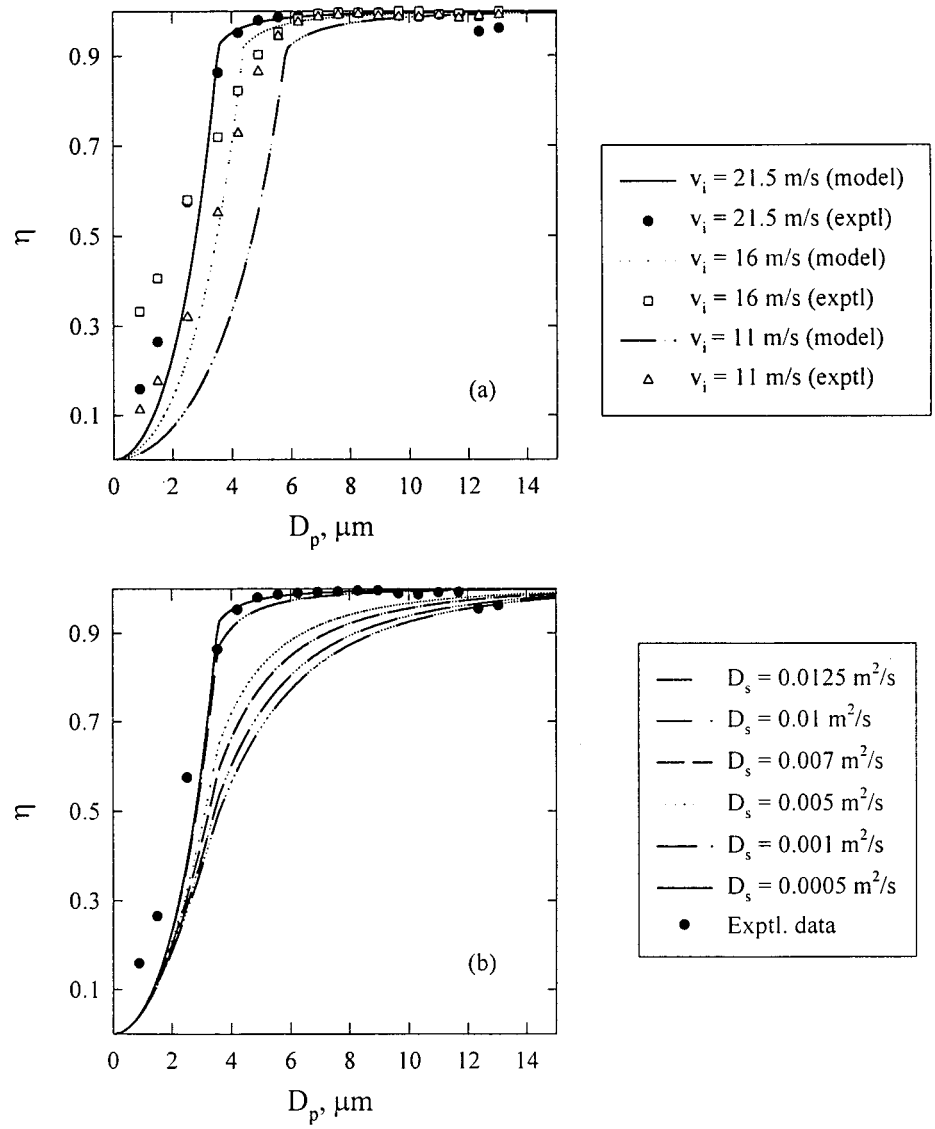

Figure 1. Grade efficiency predicted by the Mothes–Löffler[8] model and (a) its comparison with experimental results. (b) Effect of particle diffusivity (D_s) on the predicted grade efficiency (inlet velocity = 21.5 m/s).

of *Nab*, which, in turn, is proportional to the total sheet-metal area, πDHN, for geometrically similar cyclones). To account for the cost of cyclones having nonstandard geometry resulting from optimization, these correlations were modified slightly so as to relate the contribution of the fixed cost to C_o in terms of the (approximate) sheet-metal area, πDHN. Here, N identical cyclones are used in parallel to process the given feed stream. The exact equations used are included in Table 2 (eqs A26–A32). Thus, the *complete* set of model equations for the estimation of η_o, Δp, and C_o is given in Table 2. A schematic diagram showing all of the dimensional parameters of standard reverse-flow cyclone is presented in Figure 2.

To illustrate the multiobjective optimization of a train of N cyclones *at the design stage*, a feed must first be specified. The feed to be processed is described in Table 3. The feed flow rate of 165 m^3/s is the same as that used in an example provided by Benítez[34] and represents a stream to be processed in a paper mill. The average particle density, ρ_s, is 1600 kg/m^3. The viscosity of the gas is 24.8×10^{-6} Pa s. The value of D_s for this case has been assumed to be the same as that in Table 1.

Several multiobjective optimization problems with constraints can now be formulated. We illustrate the methodolgy used by selecting two objective functions, I_1 and I_2, in this work, because it is easier to study such problems and because they are often sufficient. The results for such problems can also be described visually in a more convenient manner, viz., in terms of two-dimensional plots of I_2 vs I_1. We start with Problem No. 1. An obvious choice of one objective function is the maximization of the overall collection efficiency, η_o. The natural choice for the second objective function is the minimization of the pressure drop, Δp. Several decision variables and constraints, commonly used in design, can be used. Problem No. 1 can, thus, be described mathematically as follows:

Problem No. 1

$$\text{Max } I_1(\mathbf{u}) \equiv I_1\left(N, D, \frac{D_e}{D}, \frac{B}{D}, \frac{H}{D}, \frac{S}{D}, \frac{h}{D}, \frac{a}{D}, \frac{b}{D}\right) = \eta_o \quad (3a)$$

$$\text{Min } I_2(\mathbf{u}) \equiv I_2\left(N, D, \frac{D_e}{D}, \frac{B}{D}, \frac{H}{D}, \frac{S}{D}, \frac{h}{D}, \frac{a}{D}, \frac{b}{D}\right) = \Delta p \quad (3b)$$

Table 2. Complete Set of Model Equations for Estimating η_o, Δp, and C_o

Grade and Overall Efficiency[8]

$$c_1(z) = c_0 \exp\left[-\frac{2\pi r_a^* w(r_a^*)(z - a/2)}{Q}\right] \quad \text{(A-1)}$$

$$c_3 = \frac{c_2(l) + \dot{m}_w/\left(Q\frac{H-l}{H-S}\right)}{1 + w(r_a^*)2\pi r_a^*(H-l)/\left(Q\frac{H-l}{H-S}\right)} \quad \text{(A-2)}$$

$$c_2(z) = R_1\left(\frac{H-z}{H-S}\right)^{m_1} + R_2\left(\frac{H-z}{H-S}\right)^{m_2} \quad \text{(A-3)}$$

$$c_4(z) = R_1\left(\frac{m_1 - A}{B}\right)\left(\frac{H-z}{H-S}\right)^{m_1} + R_2\left(\frac{m_2 - A}{B}\right)\left(\frac{H-z}{H-S}\right)^{m_2} \quad \text{(A-4)}$$

$$m_{1,2} = \frac{A+D}{2} \pm \sqrt{\left(\frac{A+D}{2}\right)^2 - (AD - BC)} \quad \text{(A-5)}$$

for $w(D_e/2) \geq v_r(D_e/2)$

$$A = \frac{2\pi r_a^* w(r_a^*)(H-S)}{Q} + \frac{2\pi\frac{D_e}{2}D_s(H-S)}{Q(r_a^* - D_e/2)} \quad \text{(A-6)}$$

$$B = -\frac{2\pi\frac{D_e}{2}D_s(H-S)}{Q(r_a^* - D_e/2)} - \frac{2\pi\frac{D_e}{2}[w(D_e/2) - v_r(D_e/2)](H-S)}{Q} \quad \text{(A-7)}$$

$$C = \frac{2\pi\frac{D_e}{2}D_s(H-S)}{Q(r_a^* - D_e/2)} \quad \text{(A-8)}$$

$$D = B - 1 \quad \text{(A-9)}$$

for $w(D_e/2) < v_r(D_e/2)$

$$A = \frac{2\pi r_a^* w(r_a^*)(H-S)}{Q} - \frac{2\pi\frac{D_e}{2}[w(D_e/2) - v_r(D_e/2)](H-S)}{Q} + \frac{2\pi\frac{D_e}{2}D_s(H-S)}{Q(r_a^* - D_e/2)} - 1 \quad \text{(A-10)}$$

$$B = -\frac{2\pi\frac{D_e}{2}D_s(H-S)}{Q(r_a^* - D_e/2)} \quad \text{(A-11)}$$

$$C = \frac{2\pi\frac{D_e}{2}D_s(H-S)}{Q(r_a^* - D_e/2)} - \frac{2\pi\frac{D_e}{2}[w(D_e/2) - v_r(D_e/2)](H-S)}{Q} \quad \text{(A-12)}$$

$$D = B - 1 \quad \text{(A-13)}$$

boundary conditions

$c_2(S) = c_1(S)$

$c_4(l) = c_3$

constants in the general solution

$$R_1 = c_1(S) - R_2 \quad \text{(A-14)}$$

$$R_2 = \frac{c_1(S) + F/\left[\left(\frac{H-l}{H-S}\right)^{m_2}\left(1 - \frac{E(m_1 - A)}{B}\right)\right]}{1 - \left(\frac{B - E(m_2 - A)}{B - E(m_1 - A)}\right)/\left(\frac{H-l}{H-S}\right)^{m_1 - m_2}} \quad \text{(A-15)}$$

$$F = \dot{m}_w/\left(Q\frac{H-l}{H-S}\right) \quad \text{(A-16)}$$

$$E = 1 + w(r_a^*)2\pi r_a^*(H-l)/\left(Q\frac{H-l}{H-S}\right) \quad \text{(A-17)}$$

grade efficiency, η

$$\eta = 1 - \frac{c_4(S)}{c_0} \quad \text{(A-18)}$$

overall collection efficiency

$$\eta_o = \frac{\int_0^\infty m_{in}\eta \, dD_p}{\int_0^\infty m_{in} \, dD_p} \quad \text{(A-19)}$$

Pressure drop[13]

Shepherd–Lapple model

$$\Delta H = \frac{16ab}{D_e^2} \quad \text{(A-20)}$$

Stairmand model

$$\Delta H = 1 + 2\Phi^2\left(\frac{2(D-b)}{D_e} - 1\right) + 2\left(\frac{4ab}{\pi D_e^2}\right) \quad \text{(A-21)}$$

$$\Phi = \frac{\sqrt{\frac{D_e}{2(D-b)} + \frac{4GA}{ab}} - \sqrt{\frac{D_e}{2(D-b)}}}{\frac{2GA}{ab}} \quad \text{(A-22)}$$

$G = 0.005$

$$A = \frac{\pi}{4}(D^2 - D_e^2) + \pi DH + \pi D_e S + \frac{\pi}{2}(D+B)\left[(H-h)^2 + \left(\frac{D-B}{2}\right)^2\right]^{1/2} \quad \text{(A-23)}$$

$$\Delta H = 20\left\{\frac{ab}{D_e^2}\right\}\left\{\frac{(S/D)}{[(H/D)(h/D)(B/D)]}\right\}^{1/3} \quad \text{(A-24)}$$

$$\Delta p = \frac{9806.38\Delta H \rho_g v_i^2}{9.8\rho_l} \quad \text{(A-25)}$$

Cost[32,33]

single cyclone

$$EC = \pi 575.066DH \quad \text{(A-26)}$$

multiple cyclones

$$C_{eq} = \pi 55.704DHN_c + 72N_c \quad \text{(A-27)}$$

$$C_{tci} = 2(1 + r_f)C_{eq} \quad \text{(A-28)}$$

$$C_{cr} = r_{crf}C_{tci} \quad \text{(A-29)}$$

$$P = \frac{\Delta pQ}{1000\eta_f} \quad \text{(A-30)}$$

$$C_{ann} = Ph_yC_{el} \quad \text{(A-31)}$$

total annual cost

$$C_o = C_{cr} + C_{ann} \quad \text{(A-32)}$$

subject to (s.t.)

$$15.0 \leq v_i \leq 30.0 \text{ m/s} \quad \text{(3c)}$$

$$u_i^l \leq u_i \leq u_i^u \quad \text{for } i = 1, 2, ..., 9 \quad \text{(3d)}$$

$$\text{model equations (Table 2)} \quad \text{(3e)}$$

Nine decision variables, u_i, where $i = 1, 2, ..., 9$, have been used in this problem. The number, N, of cyclones is to be taken as an integer. The constraints on the inlet velocity, v_i, are those normally used[35,36] in industrial practice. The lower bound on v_i helps ensure reasonably high values of η_o, while the upper bound helps reduce

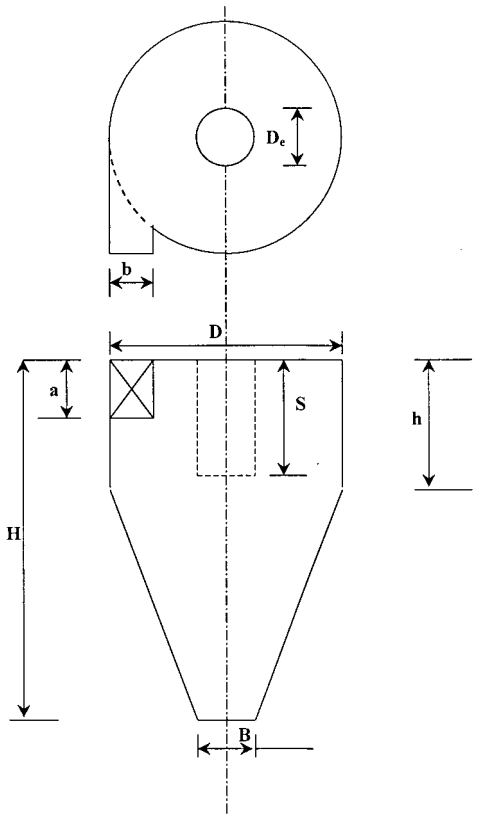

Figure 2. Schematic diagram of a cyclone.

Table 3. Feed Processed by the Cyclone To Be Optimized

Feed Specifications			
Q, m^3/s		165	
D_p, μm		10.0	
σ_p[a]		2.5	
Properties and Parameters			
ρ_g, kg/m^3	0.7895	ρ_s, kg/m^3	1600
μ_g, Pa s	24.8×10^{-6}	D_s, m^2/s	10^{-3}

[a] Log-normal size distribution of solids in feed (see Table 1).

Table 4. Bounds On Decision Variables, u_i [Problem No. 1 (reference run) as well as Problem No. 2]

First-Level (a priori) Bounds				
i	u_i	u_i^l	u_i^u	Stairmand[7] high-efficiency[a]
1	N	1	2048	
2	D, m	0.3	0.7	
3	D_e/D	0.4	0.6	0.5
4	B/D	0.325	0.425	0.375
5	H/D	3.5	4.5	4.0
6	S/D	0.4	0.6	0.5
7	h/D	1.1	1.3	1.2
8	a/D	0.4	0.6	0.5
9	b/D	0.15	0.25	0.2

Second-Level (overriding) Bounds

(i) $0.4 \le a/D \le S/D$ in any chromosome
(ii) If $0.5 \le D_e/D \le 0.6$ in any chromosome, then $0.15 \le b/D \le (1 - D_e/D)/2$

[a] Values for the Stairmand[7] high-efficiency cyclone.

problems of erosion, excessively high values of Δp, and re-entrainment of solids. Several lower (u_i^l) and upper (u_i^u) bounds have been provided for the decision variables, u_i. These are given in Table 4 and discussed later.

An alternate, two-objective optimization problem (Problem No. 2) can also be studied. In this problem, η_o is maximized while the cost, C_o, is minimized.

Problem No. 2

$$\text{Max } I_1(\mathbf{u}) \equiv I_1\left(N, D, \frac{D_e}{D}, \frac{B}{D}, \frac{H}{D}, \frac{S}{D}, \frac{h}{D}, \frac{a}{D}, \frac{b}{D}\right) = \eta_o \quad (4a)$$

$$\text{Min } I_2(\mathbf{u}) \equiv I_2\left(N, D, \frac{D_e}{D}, \frac{B}{D}, \frac{H}{D}, \frac{S}{D}, \frac{h}{D}, \frac{a}{D}, \frac{b}{D}\right) = C_o \quad (4b)$$

s.t.

$$15.0 \le v_i \le 30.0 \text{ m/s} \quad (4c)$$

$$u_i^l \le u_i \le u_i^u \quad \text{for } i = 1, 2, ..., 9 \quad (4d)$$

$$\text{model equations (Table 2)} \quad (4e)$$

The bounds used (first level or a priori bounds) on the nine decision variables, **u**, for both Problem No. 1 and Problem No. 2, are given in Table 4. Most of these have been chosen to encompass the values corresponding to the high-efficiency cyclone of Stairmand,[7] which are also provided for comparison in the table. It is hoped that our study will produce more optimal cyclone geometries than the one proposed (empirically) by Stairmand. A reasonably large range is provided for the first decision variable, N. The optimal number of cyclones to be used for the specified feed is to be computed by the optimization algorithm and should lie within the bounds (otherwise, a higher value of the upper bound should be used). Similarly, a small range for the cyclone diameter, D, of 0.3−0.7 m has been taken. The lower limit helps prevent re-entrainment of the collected solids from the cyclone wall. The upper bound on D, as for the case of N, is somewhat arbitrarily selected and has to be relaxed, at least to some extent, if the optimal solution lies at the upper bound.

An interesting requirement arises in the study of cyclone optimization. Several additional bounds and constraints must be added to override the *random* choice of decision variables. These are referred to as second-level or overriding constraints, and two that are operative for the selections made for the a priori bounds in Table 4 are mentioned in that table (additional, similar overriding constraints may need to be added for other choices). For example, both S/D and a/D have been selected to lie in the range from 0.4 to 0.6. However, a well-known practice is to have $a \le S$, as this minimizes the short-circuiting of the feed stream to the outlet. In Table 4, therefore, S/D has been allowed to be selected randomly between 0.4 and 0.6 for any chromosome, but a/D has to be governed by the overriding constraint, $0.4 \le a/D \le u_8^u$, where the value of u_8^u to be used is the value of S/D *for that particular chromosome*. In other words, the bound is chromosome-specific. Similarly, the width, b, of the rectangular inlet duct should not be such that the tangentially entering gases impinge on the outer walls of the gas-outlet pipe. Because D_e/D is allowed to take on any value (randomly) in the range 0.4−0.6, and because an a priori bound on b/D of 0.15−0.25 has been selected, it is necessary to override the latter by $0.15 \le b/D \le (1 - D_e/D)/2$, if the value of D_e/D for any particular chromosome has been chosen such that $0.5 \le D_e/D \le 0.6$ (and to use $0.15 \le b/D \le 0.25$ if $0.4 \le D_e/D \le 0.5$). The presence of these kinds of overriding bounds necessitates adaptation of the mapping procedures for the binary chromosomes into real numbers in the SGA and NSGA procedures[30] (see

Appendix) currently in use.[24,27−31] One must, for example, first map u_i for $i = 1, 2, ..., 7$ using the normal techniques. The values of S/D and D_e/D chosen for any chromosome must then be used to decide the bounds to be used for that chromosome while the binary values of a/D and b/D are mapped into the real-number domain. It must be mentioned here that the use of chromosome-specific bounds does lead to a change in the basic character of the GA. The reason for the success of the crossover operator in this algorithm is believed to be that the daughters inherit the good features of the parents. This is affected by the use of the empirical method proposed. An alternate method for dealing with this issue would be to use the penalty method, which would slowly (or instantaneously) kill the daughter chromosomes violating the above constraints. The results obtained using the latter approach were quite similar to those obtained with the present method, and this somewhat justifies the use of this empirical mapping technique. A similar inference was drawn in our earlier study[37] on the multiobjective optimization of steam reformers.

It might be mentioned that the codes for SGA and NSGA usually work with minimization of objective functions. Because one of our two objective functions in our problems in eqs 3 and 4 involves maximization, we convert our problems into pure minimization problems by defining fitness functions, F_1 and F_2, both of which are to be minimized. A common procedure[28] is to use the following:

Problems Nos. 1, 2

$$\text{Min } F_1 \equiv \frac{1}{1 + I_1} \tag{5a}$$

$$\text{Min } F_2 \equiv I_2 \tag{5b}$$

s.t.

$$\text{all earlier constraints (eqs 3 or 4, c−e)} \tag{5c}$$

The procedure used to satisfy the constraint on the range of values for v_i (eqs 3c and 4c) is to penalize chromosomes violating these constraints by adding an arbitrarily large number, P_e, to the two fitness functions, F_1 and F_2, so that such chromosomes become unfit and die out (instantaneous killing). The use of penalties does, in fact, hamper the success of a GA to some extent. A larger number of generations is required for convergence to be attained, and, possibly, some scatter and oscillations are introduced. However, constraints that cannot be easily be satisfied in an a priori manner are quite commonly encountered in chemical engineering problems of industrial interest, and we have had reasonable success in using the penalty function with GAs in recent years, as discussed in our recent review.[38]

Results and Discussion

The multiobjective optimization problems (eqs 3 and 4) were solved using a computer code for NSGA (with the adaptations of , e.g., chromosome-specific bounds and penalty functions). This code was tested earlier by our group on several multiobjective optimization problems.[38] The computational parameters[29,30] used in this study are given in Table 5. The CPU time required for the solution of the present problem was 0.24 s on a Cray J916 computer.

Table 5. Computational Parameters[29,30]

maximum number of generations, maxgen	500
population size, N_p	100
probability of crossover, p_c	0.65
probability of mutation, p_m	0.001
random seed[28]	0.87619
spreading parameter, σ	0.015
exponent controlling the sharing effect, α	2

The results of the reference ("ref") Problem No. 1 (eq 3), called Problem 1, Case 1, are shown in Figure 3 (solid circles). Some scatter is observed for the optimal values of the decision variables. Such scatter is common[38] in the solutions of complex multiobjective optimization problems as obtained by the adapted versions of NSGA. This scatter can possibly be reduced to some extent by changing the computational parameters (an expensive and possibly unnecessary step), but cannot be eliminated completely. Pareto sets are indeed obtained for the present problem.

It is interesting to observe from Figure 3 that the optimal values of the decision variables (all except N) lie at their bounds (H/D at its upper bound, all others at their lower bounds). The selection of the bounds of the geometrical ratios as the optimal values of the decision variables by the algorithm can be explained physically. For example, the overall collection efficiency generally increases with the height of the cyclone, the maximum height being limited only by the available headroom (not specified in our problem). Also, in tall cyclones, the re-entrained dust has a better chance of recollection because of the greater distance between the dust and the gas outlet. Thus, to increase the collection efficiency, the method selects H/D at its upper bound. The method selects the lower bound of B/D as the optimum value. A lower value of B/D ensures a conical structure of the cyclone and facilitates the collection of the separated dust into the hopper. It also prevents the re-entrainment of the collected dust in the hopper (the model of Mothes and Löffler[8] incorporates a region of mass transfer in which re-entrainment of deposited particles from the hopper into the lower part of the cyclone occurs). In a separate study conducted by our group,[39] we tested a 0.2-m-diameter Stairmand[7] cyclone having three different diameters (0.053, 0.075, and 0.10 m) of the vortex finder. The efficiency increases considerably with decreasing diameter of the vortex finder, although the trend indicates the presence of an optimum value. An optimum value of D_e/D in the present study lies between 0.33 and 0.5, as suggested by Dirgo and Leith.[40]

Figure 3c indicates that the values of η_o are constrained by the upper bound of 30 m/s being attained by the inlet velocity. Also, the lower bound on v_i is observed to determine the largest value of N. The sensitivity of the optimal solutions to N, from among the several decision variables used, is clearly indicated in Figure 3b. A similar sensitivity of the optimal solutions to only one or two of the decision variables has also been observed in several earlier studies[38] and is a result of the tremendous amount of "freedom" present in the optimization problem. In fact, we solved eq 3 using only one (N) or two decision variables (N and D, N and D_e/D, etc.), and it was found that the decision variables did, indeed, vary over the points on the Pareto set in these problems with considerably reduced amounts of freedom.

The results in Figure 3 indicate that the geometry of the high-efficiency cyclone suggested by Stairmand[7] on

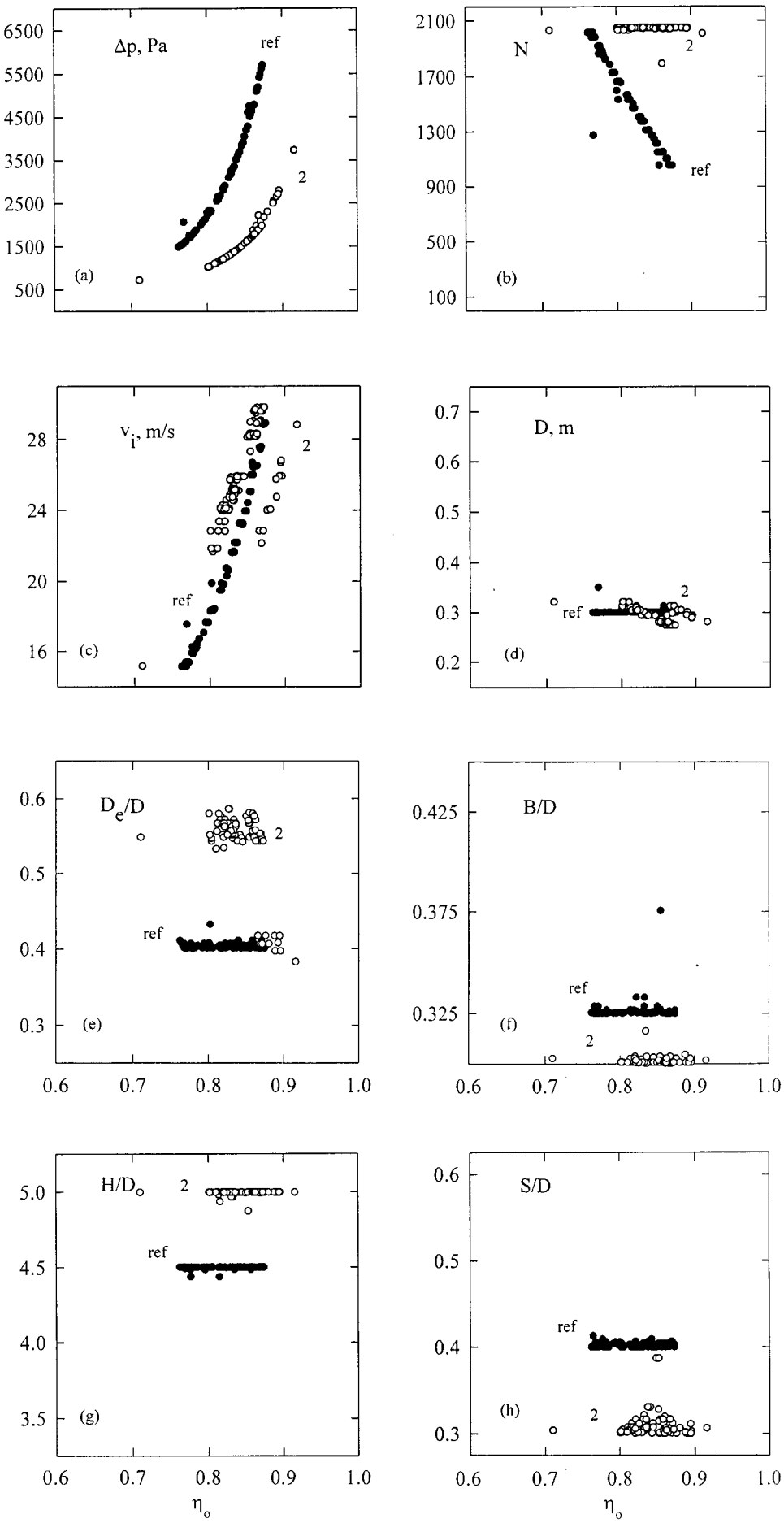
Δp, Pa
ref
2
(a)
N
2
ref
(b)
v_i, m/s
2
ref
(c)
D, m
2
ref
(d)
D_e/D
2
ref
(e)
B/D
ref
2
(f)
H/D_o
2
ref
(g)
S/D
ref
2
(h)
η_o
η_o

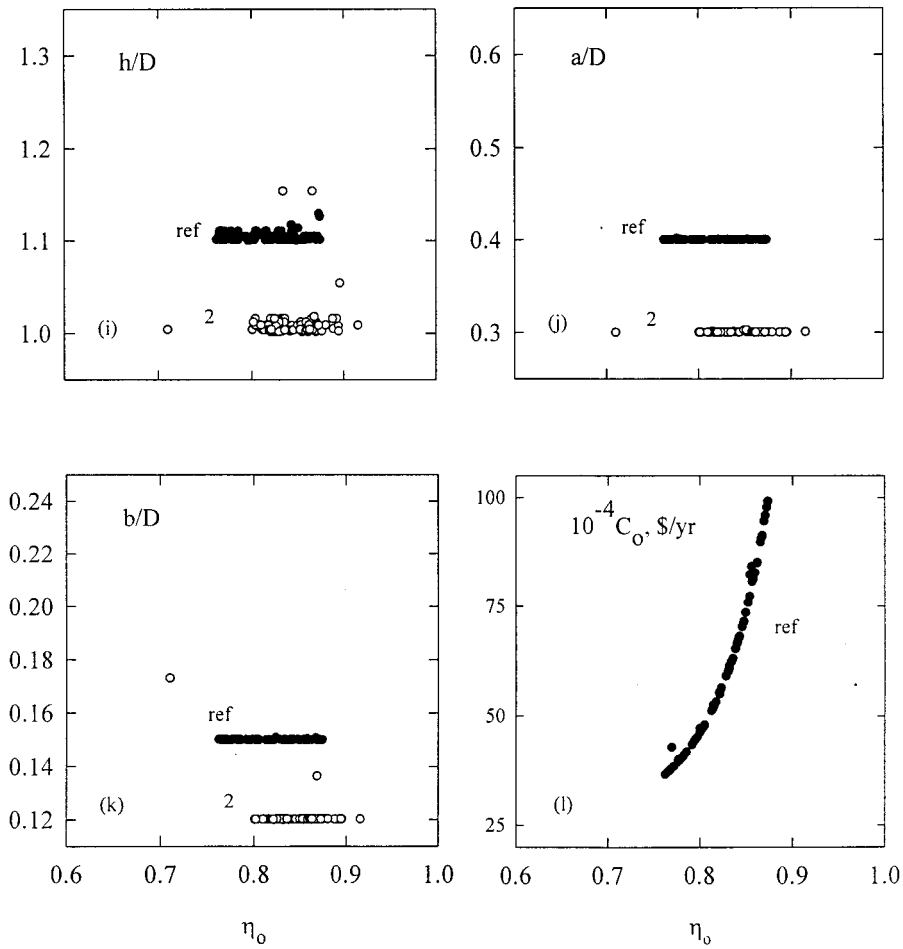

Figure 3. Optimal solutions for (●) the reference case (Problem 1, Case 1) and (○) Case 2 (Table 6). The computed values of v_i and of the cost for the points on the Pareto set are shown in panels c and l, respectively.

Table 6. Description of the Problems Studied

case #	1 (ref, Prob 1)	2 (Prob 1)	3 (Prob 1)	4 (Prob 1)	5 (Prob 2)
N	1−2048	1−2048	1−2048	1−2048	1−2048
D, m	0.3−0.7	0.2−0.7	0.3−0.7	0.3−0.7	0.3−0.7
D_e/D	0.4−0.6	0.3−0.6	0.4−0.6	0.4−0.6	0.4−0.6
B/D	0.325−0.425	0.3−0.425	0.325−0.425	0.325−0.425	0.325−0.425
H/D	3.5−4.5	3.5−5.0	3.5−4.5	3.5−4.5	3.5−4.5
S/D	0.4−0.6	0.3−0.6	0.4−0.6	0.4−0.6	0.4−0.6
h/D	1.1−1.3	1.0−1.3	1.1−1.3	1.1−1.3	1.1−1.3
a/D	0.4−0.6	0.3−0.6	0.4−0.6	0.4−0.6	0.4−0.6
b/D	0.15−0.25	0.12−0.25	0.15−0.25	0.15−0.25	0.15−0.25
v_i^l, m/s	15	15	15	15	15
v_i^u, m/s	30	30	30	30	30
Δp, Pa	–	–	0−3000	–	–
notes	–	–	–	different models[a] for Δp	cost Pareto

[a] (a) model of Stairmand[7] and (b) model of Ramachandran et al.[21]

the basis of empirical results is really not the optimal. Figure 3l gives the *computed* value of the cost, C_o, corresponding to different points on the Pareto set for the reference case (note that Figure 3l is *not* the Pareto set corresponding to Problem No. 2 described in eq 4).

A few additional problems similar to Problem No. 1 (Case 1, reference case) were also studied. Because most of the decision variables in the reference case were found to lie at either their upper or lower bounds, we decided to change all of these bounds. The details are given in Table 6 (Problem No. 1, Case 2). Figure 3 shows that the Pareto set shifts to higher values of η_o when the bounds are moved farther away from the Stairmand[7] values. Once again, the geometrical ratios B/D, H/D, S/D, h/D, a/D, and b/D are found to lie at their *new* bounds (H/D at its upper bound, all others at their lower bounds). *It appears* that η_o could be increased even more by moving the bounds further, if this is at all practically attainable. The other three decision variables, N, D, and D_e/D, corresponding to the different points on the Pareto optimal set are shown in panels b, d, and e, respectively, of Figure 3. N and D_e/D are observed to be almost constant (with some scatter in the latter), whereas D takes on values away from its new lower bound, in contrast to what was observed for the reference case. D decreases, and v_i increases, as η_o goes up. Once v_i

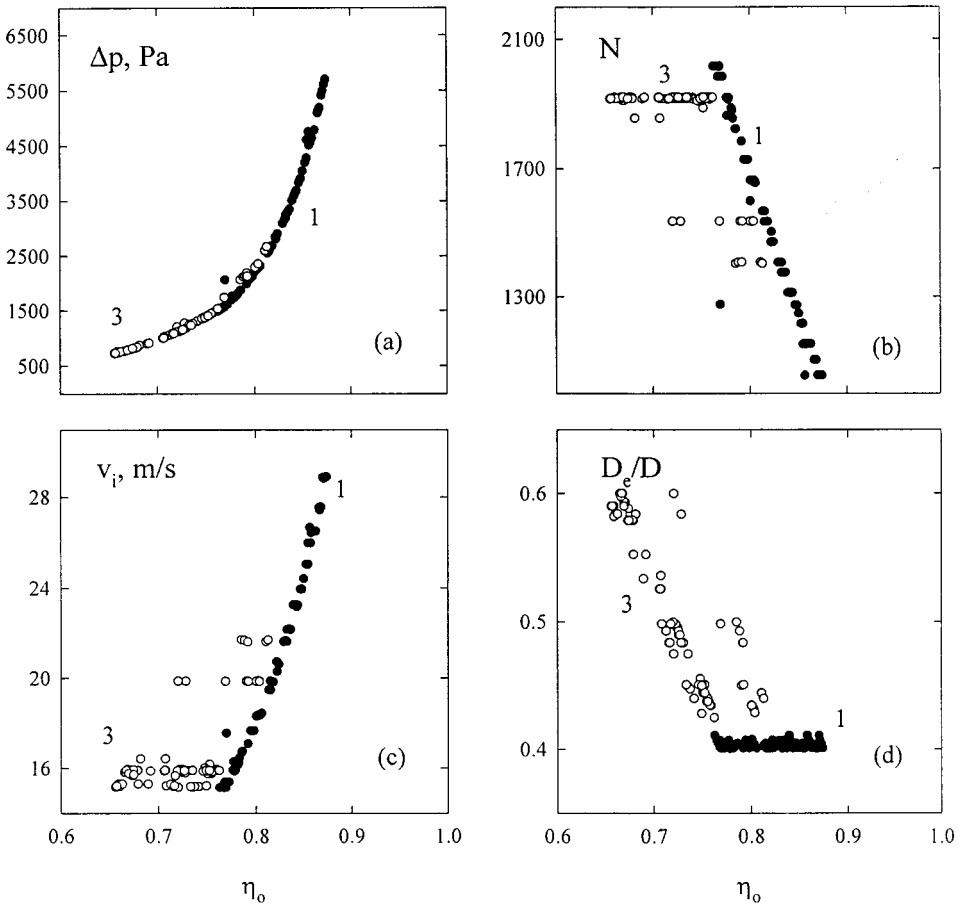

Figure 4. Optimal solutions for (○) Case 3. Results for the reference problem (Problem 1, Case 1) are also shown (●) for comparison.

reaches its upper bound, D_e/D drops suddenly, and D jumps up to give a further increase in η_o. After this jump, D_e/D again remains almost constant, and D decreases (with N constant and v_i increasing). Jumps in the values of the decision variables when a bound or constraint is reached are quite common in complex problems and, in fact, can be intuitively explained from the solutions of simpler optimization problems involving only a few decision variables.

Another variation of Problem No. 1, Case 1, is described as Case 3 in Table 6. This differs from the reference Case 1 in that an upper bound of 3000 Pa is imposed on the pressure drop. A penalty value, P_e (see discussion following eq 5) is added to the fitness functions to ensure that this constraint is satisfied. Figure 4 presents the results and compares them with those for the reference case. The effect of the reduced flexibility in Case 3 because of the constraint imposed on the pressure drop has interesting consequences on certain parameters of the cyclone. These can be observed in Figure 4b−d. D_e/D shows a decreasing trend from its maximum value of 0.6 to its minimum value of 0.4, whereas D, B/D, S/D, h/D, a/D, and b/D remain constant at their lower bounds (not shown) and H/D at its upper bound. Once D_e/D reaches its lowest value, a sudden jump occurs, with a simultaneous decrease of N and increase in v_i. The dominance of D_e/D over the other decision variables is clearly seen in this case. In passing, we mention that a large range of variation was used for the geometrical ratios in this work. It is presumed that the physical models of collection efficiency and pressure drop apply for such designs.

The effects of varying the *system* parameters, $\bar{D}_p$, σ_p, ρ_s, and Q, have also been studied, but the detailed results are not presented for the sake of brevity. It was found that increasing $\bar{D}_p$ and ρ_s and lowering σ_p shift the Pareto sets to higher values of η_o. The Pareto sets for three different values of the input gas flow rate, Q, are found to be the same. All that is required for higher values of Q is to have correspondingly larger values of N. The values of D and the geometrical ratios remain almost unchanged at their bounds, as for the reference case.

The effects of the computational parameters on the results are presented in Figure 5 for Problem No. 1. This diagram shows the distribution of the *feasible* solutions (those satisfying the constraint for the inlet velocity) at different generations. An essentially random distribution of feasible solutions is observed in the early (N_g = 1−5) generations. The Pareto set starts emerging from about the fifth generation. Figure 5g,h shows that, by about the 200th generation (N_g = 200), optimization is essentially complete. It must be emphasized that, in the early stages of NSGA, several other chromosomes (violating the constraint on the inlet velocity) are also present in the gene pool. These provide genetic diversity in the population. In the later stages, diversity is made possible by including (and not completely "killing") the "dominated" chromosomes having higher values of the front number. Figure 6a−d describes the effect of varying the crossover (p_c) and mutation (p_m) probabilities. It can be seen that the Pareto sets obtained using different values of p_c (Figure 6a−c) are superposed (in fact, panels a and c of Figure 6 are almost identical, whereas Figure 6b is superposed with these, but its range is slightly different). Thus, the effect of p_c on the

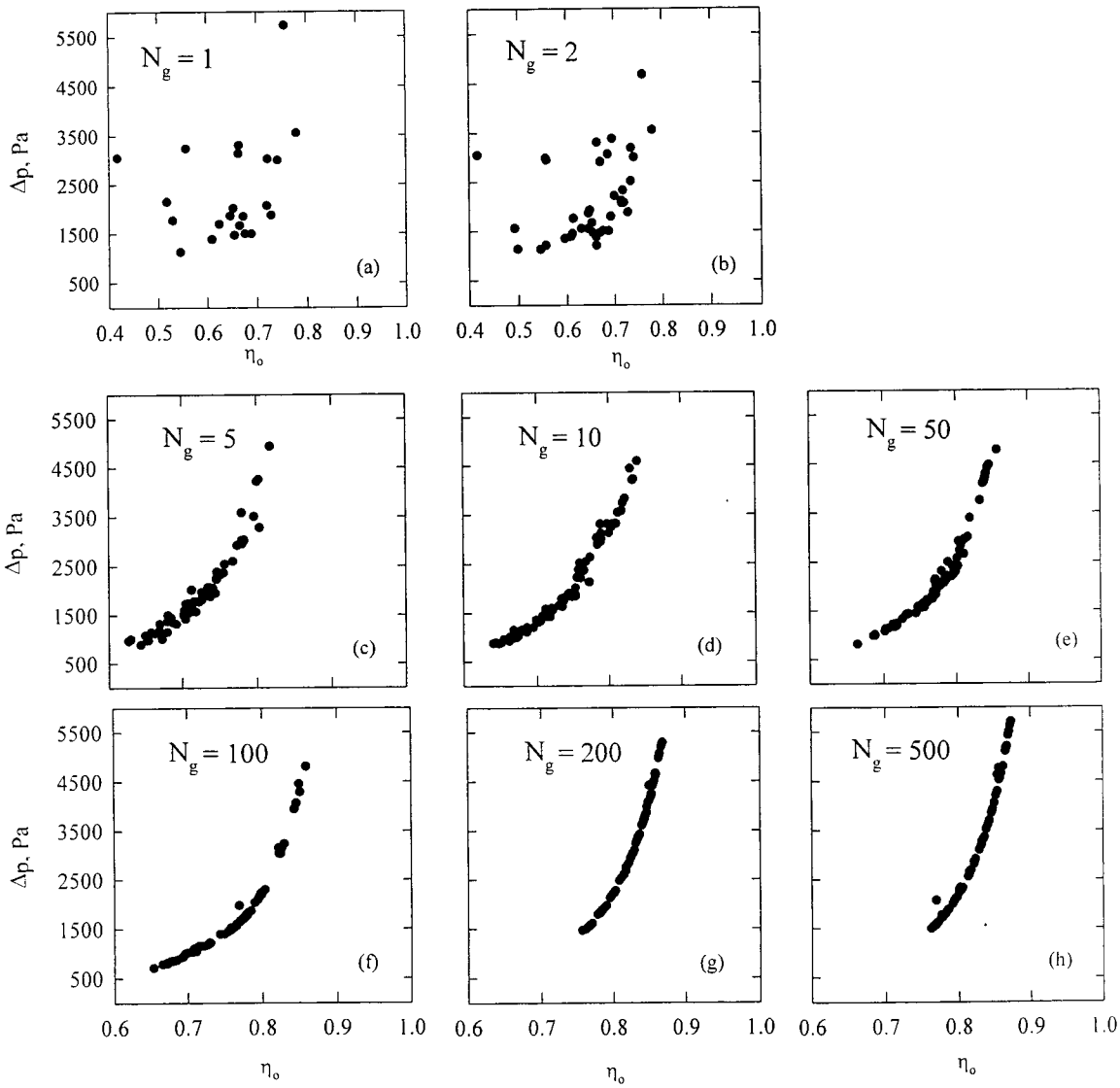

Figure 5. Development of the Pareto set (Δp vs η_o) over the generations for the reference problem (Problem 1, Case 1).

results is not too important. The same cannot be said of the mutation probability, p_m. It is seen from Figure 6d that low values of p_m result in gaps in the Pareto set. A similar effect is observed (not shown) at higher values of p_m. The best value of this computational parameter has to be found by trial. Figure 6e,f shows that the results are quite sensitive to the value of the "spreading" parameter, σ. This parameter (as well as[29,30] α) is used to decide the "closeness" of the chromosomes in the decision variable space and to help penalize chromosomes that are clustered together (hence the name). This ensures that NSGA spreads out the optimal solutions. It is observed that only a part of the Pareto set is obtained if σ is not chosen properly. Unfortunately, the choice of the best value of this parameter, too, is problem-specific.

Figure 7 shows the influence of the equations used for Δp on the Pareto set for the reference case of Problem No. 1 (Case 1). Three correlations have been used—those of Shepherd and Lapple (reference case),[13] as well as those of Stairmand[7] (Case 4a, Table 6) and Ramachandran et al.[21] (Case 4b, Table 6). The equations for Δp for all of these cases are included in Table 2. It is found that, even though the Pareto sets (Figure 7a) differ slightly, some of the important decision variables (viz., N, D, and D_e/D) are almost the same for the three cases (not shown in the figure). It is interesting to see that the optimal values of B/D and h/D are slightly different (Figure 7b,c) when the correlation of Ramachandran et al. is used (with a larger scatter for B/D).

Figure 8 gives the solution of Problem No. 2 (eq 4, Case 5 in Table 6). In this problem, the annual cost, C_o, is minimized, while η_o is maximized. The bounds of the decision variables are the same as for Case 1. D, B/D, S/D, h/D, a/D, and b/D are found to lie at their lower bounds, whereas H/D is at its upper bound. The cost Pareto in Figure 8a is found to extend over a lower range of values of η_o. Again, D_e/D is constant at its upper bound until a certain point and then jumps quite suddenly to near its lower bound (Figure 8d), whereas N decreases almost linearly and jumps up (and thereafter falls again) when D_e/D jumps down. The importance of both N and D_e/D as decision variables controlling the Pareto set for Problem No. 2 is observed. Figure 8e shows the calculated values of Δp corresponding to the different points on the C_o vs. η_o Pareto. It is interesting to observe (Figure 8e) that the Δp vs. η_o Pareto for Case 1 (Problem No. 1) is almost indistinguishable from the computed Δp vs. η_o curve corresponding to the cost Pareto over the range where the

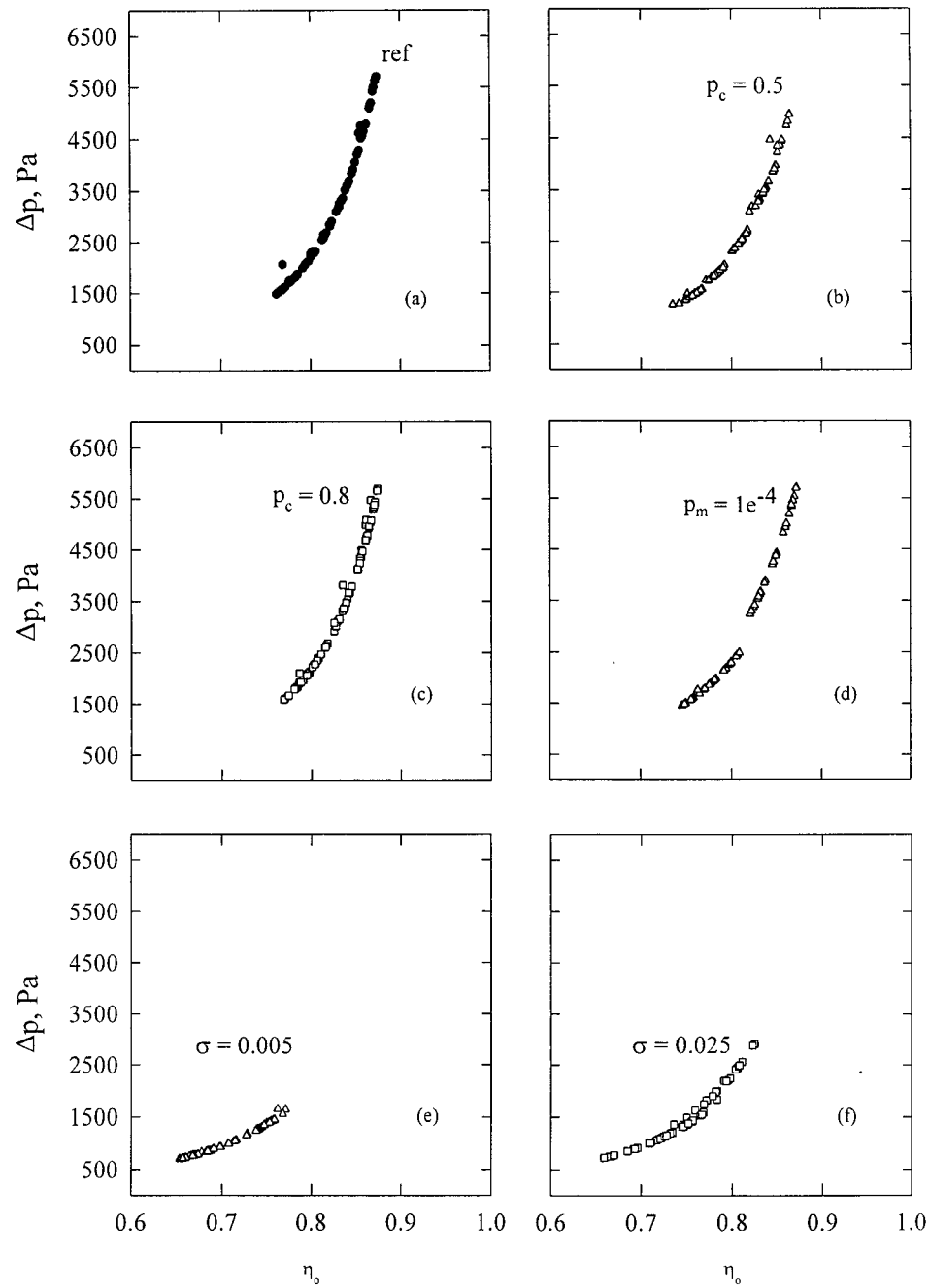

Figure 6. Effect of p_c, p_m, and σ on the Pareto set for the reference case (Problem 1, Case 1).

values of η_o are similar. Similarly, the other decision variables are superposed in this range. The parallelism between these two curves is to be noted and suggests that three-dimensional Paretos (maximize η_o, minimize Δp, minimize C_o) will not lead to substantially different results.

Conclusions

Multiobjective optimization of an industrial cyclone treating 165 m^3/s of air was carried out using the NSGA technique. A few illustrative problems that maximized the cyclone efficiency and minimized the pressure drop by altering a combination of nine decision variables were solved. The decision variables include eight geometrical parameters of a reverse-flow cyclone (D, D_e/D, B/D, H/D, S/D, h/D, a/D, and b/D) and the number of identical cyclones (N) used in parallel. It was found that D, D_e/D, and N are the important decision variables controlling the nondominated Pareto optimal solutions of collection efficiency and pressure drop. In addition, it was also observed that, whenever a bound or constraint is reached, sudden changes in the plots of the optimal values of N, D, and/or D_e/D occur. For a majority of the optimal solutions, the rest of the decision variables lie at their lower bounds, except for H/D, which lies at its upper bound. Indeed, the optimal geometry under reference conditions ($D_e/D = 0.4$, $B/D = 0.325$, $H/D = 4.5$, $S/D = 0.4$, $h/D = 1.1$, $a/D = 0.4$, $b/D = 0.15$) is found to be significantly different from the values suggested by Stairmand[7] for the high-efficiency cyclone conditions ($D_e/D = 0.5$, $B/D = 0.375$, $H/D = 4.0$, $S/D = 0.5$, $h/D = 1.5$, $a/D = 0.5$, $b/D = 0.2$).

The optimal solutions obtained by cost minimization are parallel to the solutions obtained by pressure

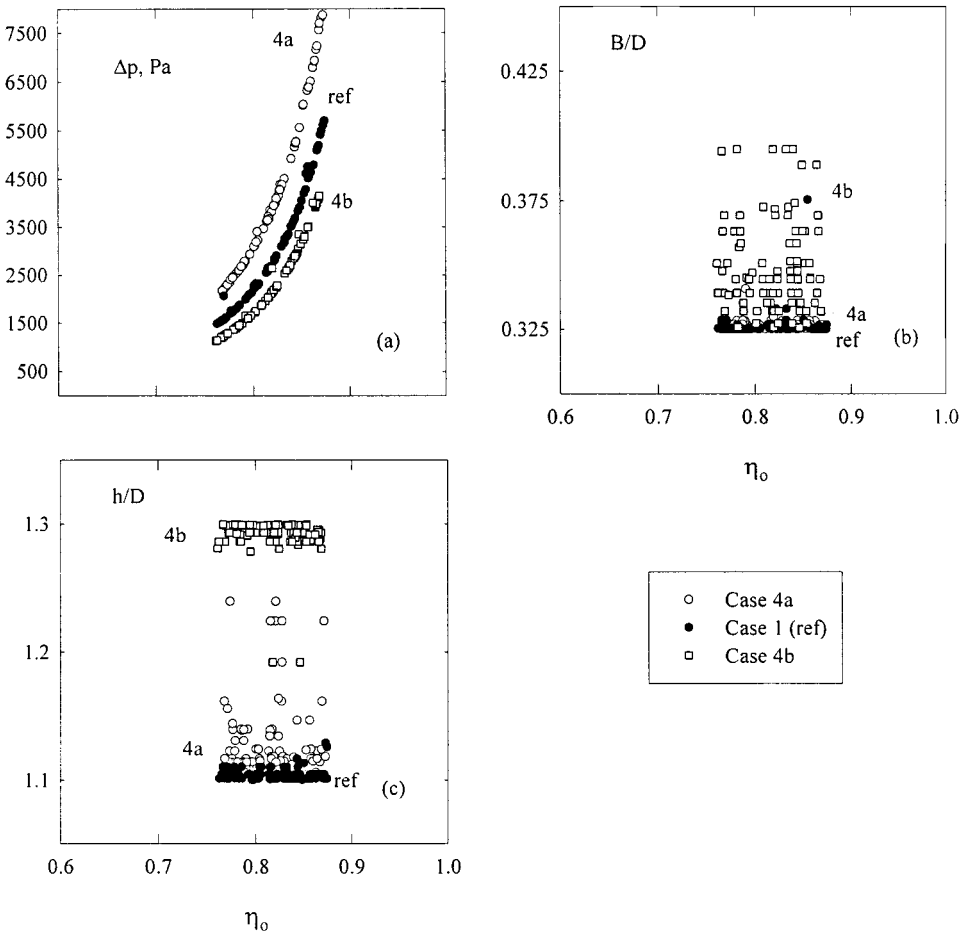

Figure 7. Results of Cases 4a and b (different models for the pressure drop). Results for the reference problem (Problem 1, Case 1) are also shown (●) for comparison.

minimization. Therefore, the three-dimensional Paretos (maximize η_o, minimize Δp, minimize C_o) are expected to lead to similar optimal values of the decision variables. The Pareto solutions obtained in this work assist in narrowing down the choices faced by the decision maker for the optimal operation of cyclones.

Appendix 1

Summary of the Simple Genetic Algorithm[24,27,28] **and NSGA.**[29,30] A genetic algorithm (GA, or simple GA, SGA) is a robust, AI-based computational technique for optimization that mimics the mechanisms of natural evolution. This is done by the creation of a population of solutions (each represented in terms of a set of several binary numbers generated randomly), referred to as chromosomes or strings. These are analogous to the chromosomes in DNA. The chromosomes then go through a process of simulated "evolution".

Each chromosome encodes the values of the different parameters (decision variables) being optimized, in terms of several binary digits (bits). Bit-manipulation operators then implement reproduction, crossover, mutation, and other biological operators of natural evolution, to improve the "fitness" of the chromosomes.

During the implementation of a GA, the binary information on decision variables is first mapped into real values using prescribed bounds, and the fitness (objective) functions of the chromosomes are evaluated using a model. A new population (generation) is created by performing reproduction of the chromosomes in the current population using the Darwinian principle of survival of the fittest. This is done by copying the chromosomes in the earlier generation into a gene pool, with the number of copies made being proportional to their fitness functions. The chromosomes in the gene pool then undergo pairwise random crossover and random mutation operations in order to provide members of the next generation. In the course of several generations, the fitness of the chromosomes improves, and fitter sets of strings emerge.

Deb and Srinivas[29] developed the nondominated sorting genetic algorithm (NSGA) to solve problems involving the optimization of multiple objectives. The algorithm generates a set of solutions and classifies these into several fronts. In any front, the chromosomes are mutually nondominating over each other [two solutions are said to be nondominating, if, on moving from one solution to another, we find an improvement in one of the objective functions but a deterioration in one (or more) of the other objective function(s)]. The chromosomes in these fronts are assigned progressively lower, common (dummy) values of the fitness function. Each chromosome in any front is then assigned an individual value of the fitness function. This is obtained by dividing the common dummy fitness value for the members of the front by the niche count of the individual chromosome. The niche count gives an indication of how dense the population is around any particular chromosome (in the decision variable space). In computing the niche count of any chromosome, the other chromosomes at the same location are counted completely (as one full

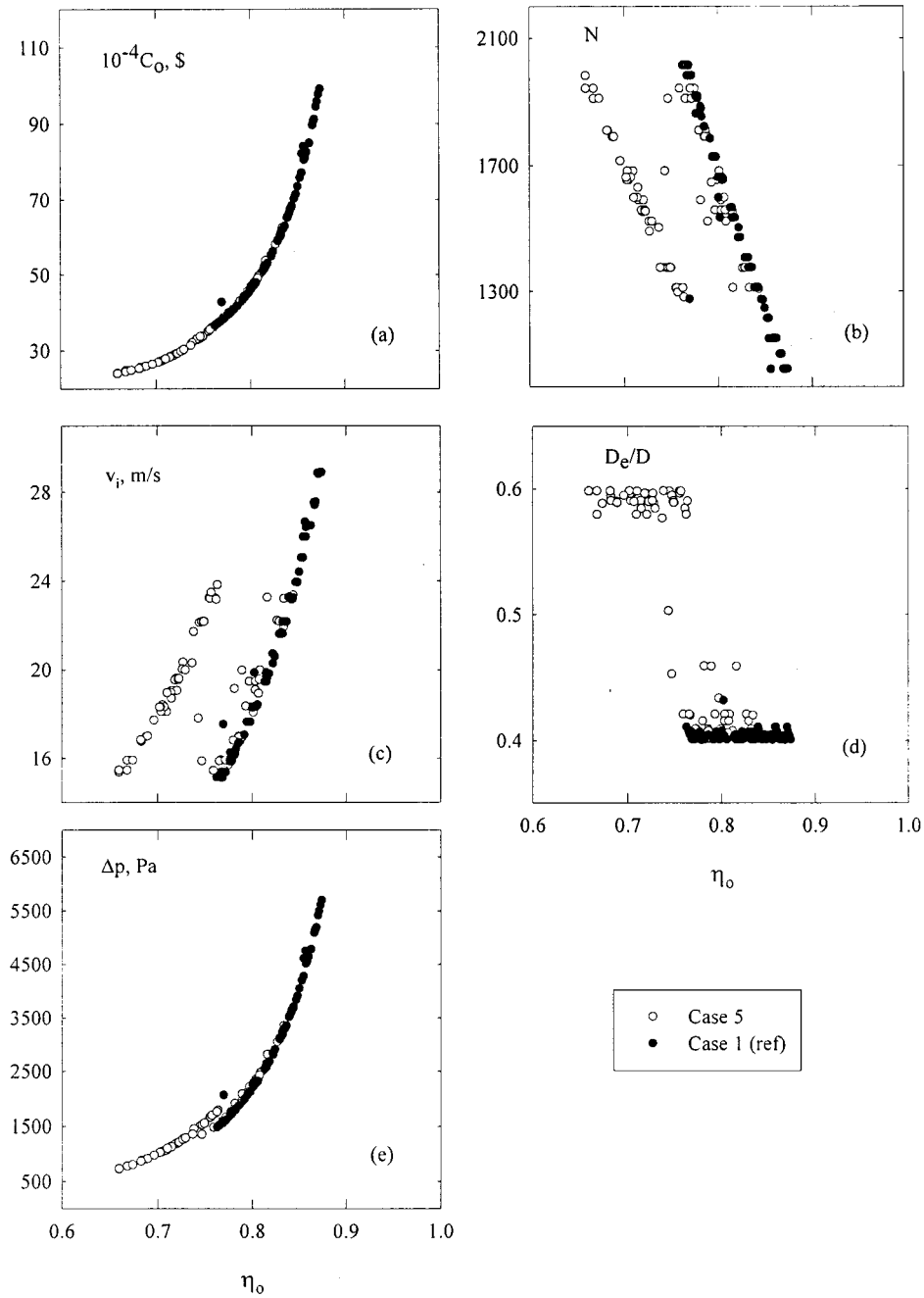

Figure 8. Optimal solutions for Case 5 (Problem No. 2, eq 4). Results for the reference problem (Problem 1, Case 1) are also shown (●) for comparison.

neighbor). The contribution of any member lying farther away is given by the expression $1 - (\text{distance}/\sigma)^{\alpha}$. Thus, the farther a neighbor happens to be, the lower its contribution to the niche count of any particular chromosome. A chromosome that is at a distance farther than σ is not counted as a neighbor. Computation of the fitness function using the niche count, referred to as sharing, helps to spread out the chromosomes, as this procedure favors chromosomes that are spaced farther apart while penalizing those that are closely clustered. At the end of this procedure, each string in the gene pool has a value of the fitness function associated with it, with the value of the fitness function being the highest for the most isolated and most highly nondominated chromosome. This is followed by the reproduction, crossover, and mutation operations, as in SGAs. A flowchart is available in refs 31 and 38.

Acknowledgment

The authors acknowledge the financial support from National University of Singapore and the advice of Dr. A. C. Hoffmann of University of Groningen, The Netherlands. One of the authors (S.K.G.) gratefully acknowledges the hospitality provided by the University of Wisconsin, Madison, where this paper was revised.

Nomenclature

a = height of the cyclone inlet (m)
A = area of the cyclone (m^2)
b = width of the cyclone inlet (m)
B = diameter of the base of the cyclone (m)
c_0, c_1, c_2, c_3, c_4 = concentration of particles (kg/m^3)
C_{ann} = total annual cost ($)
C_{cr} = capital recovery cost ($/year)

C_{el} = cost of electricity
C_{eq} = total equipment cost ($)
C_o = total cost ($/year)
C_{tci} = total capital investment ($)
d_{50} = cut diameter (μm)
D = diameter of the cyclone (m)
D_e = diameter of the exit pipe (m)
$\bar{D}_p$ = mass-mean diameter of solids (μm)
D_s = effective mean diffusivity of solids in gas (m^2/s)
$\mathbf{F}$ = fitness function
G = friction coefficient
h = height of the cylindrical portion of the cyclone (m)
H = total height of the cyclone (m)
h_y = number of hours per year
$\mathbf{I}$ = objective function
l = natural length (m)
m_{in} = mass of solid size D_p in feed
N = number of cyclones
P = power (watt)
P_e = penalty value
Q = inlet flow rate (m^3/s)
r_a* = corrected radius (m)
r_{crf} = rate of capital recovery
r_f = rate of freight and tax
S = depth of the exit pipe (m)
$\mathbf{u}$ = decision variable
v_i = inlet velocity (m/s)
v_r = radial velocity (m/s)
w = settling velocity (m/s)

Greek symbols

α = exponent controlling the sharing (spreading) effect
ΔH = number of inlet velocity heads
Δp = pressure drop (Pa)
η = grade efficiency
η_o = overall collection efficiency
μ_g = viscosity of gas (Pa.s)
ρ_g = density of gas (kg/m^3)
ρ_s = density of solids (kg/m^3)
σ = sharing (spreading) parameter
σ_p = standard deviation of size distribution of solids

Subscripts

s = solids
g = gas
l = liquid
i = decision variable

Superscripts

u = upper bound on the decision variable
l = lower bound on the decision variable

Literature Cited

(1) Barth, W. Design and Layout of the Cyclone Separator on the Basis of New Investigations. *Brennst.−Waerme−Kraft* **1956**, *8*, 1.

(2) Lapple, C. E. Gravity and Centrifugal Separation. *Ind. Hyg. Q.* **1950**, *1*, 40.

(3) Overcamp, T. J.; Scarlett, S. E. Effect of Reynolds Number on the Stokes Number of Cyclones. *Aerosol Sci. Technol.* **1993**, *19*, 362.

(4) Leith, D.; Licht, W. The Collection Efficiency of Cyclone Type Particle Collectors—A New Theoretical Approach. *AIChE Symp. Ser.* **1972**, *68*, 196.

(5) Dietz, P. W. Collection Efficiency of Cyclone Separators. *AIChE J.* **1981**, *27*, 888.

(6) Mothes, H.; Löffler, F. Investigation of Cyclone Grade Efficiency Using a Light Scattering Particle Size Measuring Technique. *J. Aerosol Sci.* **1982**, *13*, 184.

(7) Stairmand, C. J. Pressure Drop in Cyclone Separators. *Engineering* **1949**, *168*, 409.

(8) Mothes, H.; Löffler, F. Prediction of Particle Removal in Cyclone Separators. *Int. Chem. Eng.* **1988**, *28*, 231.

(9) Li, E.; Wang, Y. A New Collection Theory of Cyclone Separators. *AIChE J.* **1989**, *35*, 666.

(10) Salcedo, R. L. Collection Efficiencies and Particle-Size Distributions from Sampling Cyclones—Comparison of Recent Theories with Experimental Data. *Can. J. Chem. Eng.* **1993**, *71*, 20.

(11) Ray, M. B.; Luning, P. E.; Hoffmann, A. C.; Plomp, A.; Beumer, M. I. L. Post Cyclone (PoC): An Innovative Way to Reduce the Emission of Fines from Industrial Cyclones. *Ind. Eng. Chem. Res.* **1997**, *36*, 2766.

(12) Ray, M. B.; Hoffmann, A. C.; Postma, R. S. Performance of Different Analytical Methods in Evaluating Grade Efficiency of Centrifugal Separators. *J. Aerosol Sci.* **2000**, *31*, 563.

(13) Shepherd, C. B.; Lapple, C. E. Flow Pattern and Pressure Drop in Cyclone Dust Collectors, Cyclone without Inlet Vane. *Ind. Eng. Chem.* **1940**, *32*, 1246.

(14) Alexander, R. M. Fundamentals of Cyclone Design and Operation. *Proc. Aust. Inst. Min. Met.* **1949**, *152*, 203.

(15) First, M. W. Cyclone Dust Collector Design. *Am. Soc. Mech. Eng.* **1949**, 49-A-127.

(16) Dirgo, J. A. *Relationships Between Cyclone Dimensions and Performance*; Ph.D. Thesis, Harvard University: Cambridge, MA, 1988.

(17) Stern, A. C.; Caplan, K. J.; Bush, P. D. *Cyclone Dust Collectors*; American Petroleum Institute: New York, 1955.

(18) Leith, D.; Mehta, D. Cyclone Performance and Design. *Atmos. Environ.* **1973**, *7*, 527.

(19) Muschelknautz, E. Design of Cyclone Separators in the Engineering Practice. *Staub−Reinhalt. Luft* **1970**, *30*, 1.

(20) Dirgo, J.; Leith, D. Cyclone Collection Efficiency: Comparison of Experimental Results with Theoretical Predictions. *Aerosol Sci. Technol.* **1985**, *4*, 401.

(21) Ramachandran, G.; Leith, D.; Dirgo, J.; Feldman, H. Cyclone Optimization Based on a New Empirical-Model for Pressure-Drop. *Aerosol Sci. Technol.* **1991**, *15*, 135.

(22) Barth, W.; Leineweber, L. Evaluation and Design of Cyclone Separators. *Staub* **1964**, *24*, 41.

(23) Leineweber, L. Design of Cyclones for Given Maximum Particle Size, Pressure Loss, and Flow Rate. *Staub−Reinhalt. Luft* **1967**, *27*, 11.

(24) Holland, J. H. *Adaptation in Natural and Artificial Systems*; University of Michigan Press: Ann Arbor, MI, 1975.

(25) Chankong, V.; Haimes, Y. Y., *Multiobjective Decision Making—Theory and Methodology*; Elsevier: New York, 1983.

(26) Goicoechea, A.; Hansen, D. R.; Duckstein, L. *Multiobjective Decision Analysis with Engineering and Business Applications*; Wiley: New York, 1982.

(27) Goldberg, D. E. *Genetic Algorithms in Search, Optimization, and Machine Learning*; Addison-Wesley: Reading, MA, 1989.

(28) Deb, K. *Optimization for Engineering Design: Algorithms and Examples*; Prentice Hall of India: New Delhi, India, 1995.

(29) Srinivas, N.; Deb, K. Multiobjective Function Optimization using Nondominated Sorting Genetic Algorithms. *Evol. Comp.* **1995**, *2*, 3.

(30) Mitra, K.; Deb, K.; Gupta, S. K. Multiobjective Dynamic Optimization of an Industrial Nylon 6 Semibatch Reactor Using Genetic Algorithm. *J. Appl. Polym. Sci.* **1998**, *69*, 69.

(31) Garg, S.; Gupta, S. K. Multiobjective Optimization of a Free Radical Bulk Polymerization Reactor Using Genetic Algorithm. *Macromol. Theory Simul.* **1999**, *8*, 46.

(32) Vatavuk, W. M. *Estimating Costs of Air Pollution Control*; Lewis: Chelsea, MI, 1990.

(33) Crawford, M. *Air Pollution Control Theory*; McGraw-Hill: New York, 1976.

(34) Benítez, J. *Process Engineering and Design for Air Pollution Control*; Prentice Hall: Englewood Cliffs, NJ, 1993.

(35) Svarovsky, L. *Solid−Gas Separation*; Elsevier: Amsterdam, 1981.

(36) Gupta, S. K. *Momentum Transfer Operations*; Tata McGraw-Hill: New Delhi, India, 1979.

(37) Rajesh, J. K.; Gupta, S. K.; Rangaiah, G. P.; Ray, A. K. Multiobjective Optimization of Steam Reformer Performance using Genetic Algorithm. *Ind. Eng. Chem. Res.* **2000**, *39*, 706.

(38) Bhaskar, V.; Gupta, S. K.; Ray, A. K. Applications of Multiobjective Optimization in Chemical Engineering. *Rev. Chem. Eng.* **2000**, *16*, 1.

(39) Hoffmann, A. C.; Berrino, A.; Ray, M. B. On the Shape of Grade Efficiency Curves Computed for Centrifugal Dedusters by CFD with Lagrangian Particle Tracking. *Advanced Technologies for Particle Processing*; Vol. II, pp 63−69. Proceedings of the Topical Conference on Particle−Particle Interaction at the AIChE annual meeting, Nov 15−20, 1998, Miami Beach, FL.

(40) Dirgo, J.; Leith, D. *Encyclopedia of Fluid Mechanics*; Cheremisinoff, N. P., Ed.; Gulf Publishing Co.: Houston, TX, 1986.

Received for review October 12, 1999
Accepted July 22, 2000
IE990741C